SAND98-2444C

Electrochemical Evaluation of Pyrite Films Prepared by Plasma Spraying

Ronald A. Guidotti and Frederick W. Reinhardt
Sandia National Laboratories
Albuquerque, NM 87185-0614

and

Hui Ye, Chris Strock, T. Danny Xiao, and David E. Reisner
U.S. Nanocorp., Inc.
North Haven, CT 06473

RECEIVED
NOV 17 1998
OSTI

ABSTRACT

Thermally activated batteries use electrodes that are typically fabricated by cold pressing of powders. In the LiSi/FeS_2 system, natural (mineral) pyrite is used for the cathode. In an effort to increase the energy density and specific energy of these batteries, flame and plasma spraying to form thin films of pyrite cathodes were evaluated. The films were deposited on a 304 stainless steel substrate (current collector) and were characterized by scanning electron microscopy and x-ray diffraction. The films were electrochemically tested in single cells at 500°C and the performance compared to that of standard cells made with cold-pressed powders. The best results were obtained with material deposited by dc-arc plasma spraying with a proprietary additive to suppress thermal decomposition of the pyrite.

INTRODUCTION

The LiSi/FeS_2 (pyrite) couple is the primary power source used for thermally activated batteries ("thermal batteries"). These batteries are designed to function only when the electrolyte phase becomes molten. Until the internal pyrotechnic heat source is ignited, the batteries are inert and have an almost unlimited shelf life. Common electrolytes used for these applications include the LiCl-KCl eutectic that melts at 352°C and the all-lithium LiCl-LiBr-LiF minimum-melting electrolyte that melts at 436°C.

The cathode, separator, and anodes are typically prepared by cold pressing of powders in dies. The separator contains enough MgO (typically, 35 w/o) to act as an immobilization agent for the electrolyte once the battery has been activated and the electrolyte melts. The catholyte contains 25% or more separator material and, in many cases, 1.5% Li_2O to act as a lithiation agent to mitigate voltage transients caused by electroactive iron impurities. The anode contains 20-25% electrolyte to aid in pelletizing and to improve the electrochemical performance by increasing the ionic conductivity. Each cell in a bipolar thermal-battery stack contains pellets of anode, separator, cathode, and pyrotechnic source (typically, $Fe/KClO_4$ blends) and 304 stainless steel current collectors between the anode and the heat pellet and between the heat pellet and cathode

DISCLAIMER

of the adjacent cell. These also serve as thermal buffers to moderate the heat input to the active cell components. This is important for the FeS_2 cathode, in that FeS_2 becomes thermally unstable above 550°C, decomposing according to equation 1:

$$FeS_{2(s)} \text{ ----> } FeS_{(s)} + 0.5S_{2(g)} \qquad [1]$$

Under those conditions, the fugitive sulfur vapor can react directly with the LiSi anode to generate enough heat to cause a thermal-runaway condition where the battery self-destructs.

The need to press catholyte powders increases production costs for thermal batteries because of the high labor costs associated with processing of this material (e.g., blending, pelletizing, and quality control checks for weight and thickness). While the current technology of using cold-pressed pellets works well, it has a number of intrinsic limitations. The thinnest pellets that can be fabricated with reasonable yields range from 0.010" to 0.012" in thickness. For many applications, there is much more capacity than is actually needed due to the difficulty of fabricating and handling of very thin pellets. The use of a graphite-paper substrate to act as a reinforcing agent greatly helps with the cathode pellet. This is not an option with the separator and anode pellets, however. The use of excess material increases the overall length and mass of the thermal battery unnecessarily. If the pellet thickness were limited to the actual amount of material that is needed, a significant increase in the specific energy and energy density could be realized. Plasma spraying offers the potential to do this.

In addition to the limitations described above, pressing of large pellets becomes increasingly more difficult as the diameter of the pellet is increased from 1" to 5". The necessary pressure for compaction of pellets increases rapidly as the square of the area of the pellet, so that presses with capacities of 500 tons or more are needed for the larger pellets. This imposes a practical upper limit for pellets that can be prepared in this way. Plasma-sprayed electrodes, on the other hand, don't suffer from this limitation. If a uniform layer of pyrite could be deposited onto a substrate with adequate adhesion, parts could be punched from a sheet with a resultant reduction in cost for cathode preparation—especially for the larger-diameter batteries.

Plasma spraying of materials has a number of other potential advantages. The deposit thickness can be readily controlled from very thin films (e.g., 10 μm) to reasonably thick ones (e.g., millimeters) and a wide variety of materials are amenable to spraying. Strong adhesion would also result in reduced interfacial resistance between the current collector and the cathode which would result in a higher power output. A monolithic FeS_2 cathode would also reduce the interparticle resistance associated with pressed compacts which could further increase power capability.

In this work, we report on the preliminary results of our efforts in plasma spraying of thin (25-μm to 1-mm thick) pyrite films onto 304 stainless steel substrates. Both natural pyrite and nanostructured pyrite agglomerates were used as powder feedstock for the study. A range of spraying conditions was examined and the resulting deposits were characterized by x-ray diffraction (XRD) for phase identification. Subsequently, test coupons 1.25" in diameter were tested at several current densities at 500°C in single cells using LiSi anodes and LiCl-KCl-based separators. The electrochemical performance was compared to that of cathodes prepared by conventional techniques (cold pressing of powders) for reference purposes. This paper will present the results of that work, including a number of the problem areas that were addressed and the research and engineering work that will be necessary to make this process commercially viable.

EXPERIMENTAL

Flame/Plasma Spraying

One technique for spray deposition of material that was examined was a high-velocity oxygen flame (HVOF). A Metco Diamond Jet HVOF system was used in this work. In this method, the feed material is directly injected into a hydrogen-oxygen flame that is rapidly expanded at the nozzle exit before impinging onto the collection substrate of 0.010"-thick 304 stainless steel. A second technique evaluated was the dc-arc plasma spray, done under an argon cover (250 SCFH), with arc currents of between 200 A and 300 A. A Metco 9MB plasma spray system was used for this work. Cornstarch was added to the FeS_2 as a fugitive flow enhancer. To minimize potential oxidation of the pyrite during spraying, a protective enclosure was constructed and a cover gas of argon was used. In later tests, a proprietary additive was added to the pyrite feedstock to aid in processing and to suppress FeS_2 decomposition.

Electrochemical Testing

The plasma-sprayed pyrite samples were fabricated into 1.25"-dia. single cells with 44% Li/56 % Si (by wt.) anodes and separators based on 35% MgO and LiCl-KCl eutectic. The mass of active FeS_2 in each sample was determined to allow gravimetric efficiencies to be calculated. Control tests were performed using conventional pressed-power cathodes containing 73.5% FeS_2/25% separator/1.5% Li_2O (1.05 g, 0.018" thick). The FeS_2 particle size ranged from 35µm to 44 µm. Cells were discharged galvanostatically between heated platens at 500°C under computer control in a glovebox under an atmosphere of high-purity argon to a cutoff voltage of 0.5 V. A steady-state current of 1 A (~125 mA/cm^2) was used with a 1-s 2 A (~250 mA/cm^2) pulse applied every minute. This allowed the overall cell resistance to be determined as a function of depth of discharge. Prior to discharge, the cells were placed on open circuit for 25-30 s.

RESULTS

Performance of Natural Pyrite

The electrochemical performance of a standard $LiSi/FeS_2$ cell made with conventional pellets cold pressed from powders is shown in Figure 1, along with the corresponding cell resistance. (The resistance of the cell was calculated from the voltage drop during the pulses and included non-ohmic as well as IR contributions.) The upper plateau voltage is represented by equation 2.

$$FeS_2 + 3/2\,Li^+ + 3/2\,e^- \longrightarrow 1/2\,Li_3Fe_2S_4 \qquad [2]$$

The theoretical capacity of the FeS_2 for this reaction is 1,206 coulomb/g.

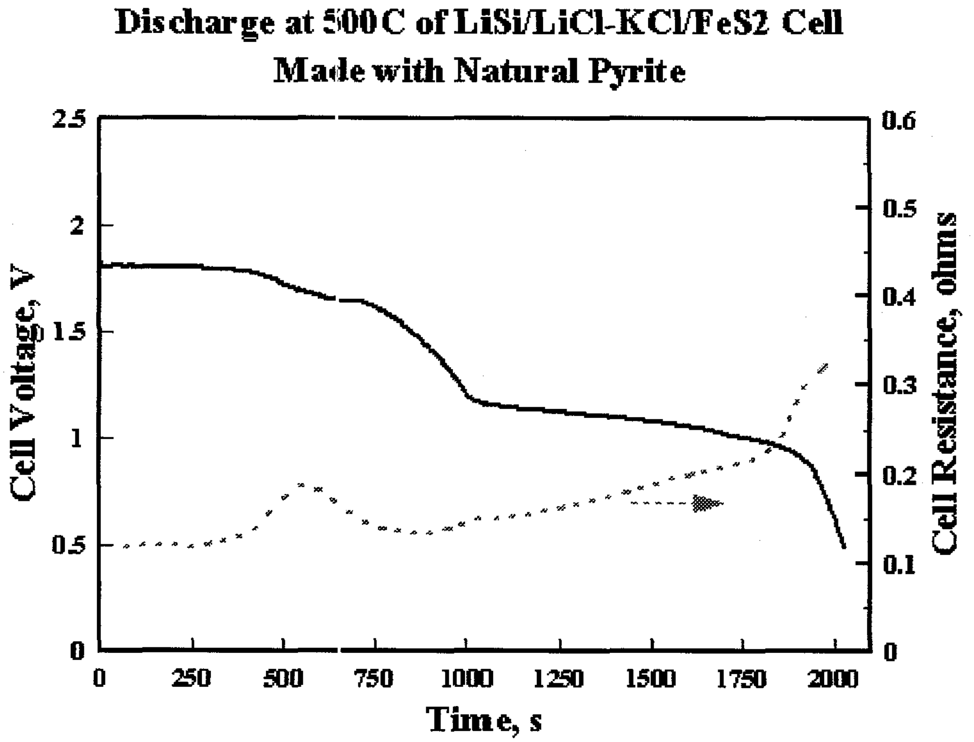

Discharge at 500C of LiSi/LiCl-KCl/FeS2 Cell Made with Natural Pyrite

Figure 1. Discharge of Conventional Pelletized LiSi/FeS_2 (Pyrite) Single Cell at 500°C at 125 mA/cm^2. 1-S Pulses of 250 mA/cm^2 Were Applied Every 60 S.

The first voltage transition starting near 480 s is due to discharge of $Li_3Fe_2S_4$ to a complex mixture of lower sulfides of iron, $Li_{2-x}Fe_{1-x}S_2$ + $Fe_{1-x}S$, where x~0.2. The much larger voltage transition near 1,000 s is related to formation of Li_2FeS_2 (Li_2S + FeS) (1,2). (These transformations were verified to be cathode related in tests that incorporated a Ag/AgCl reference electrode.) With the masses of anode and cathode used in this work, the cells were cathode limited in all cases. Hence, the anode phase transformation that occurs would not take place until well after 1,200 s.

The increase in resistance that occurs at the voltage transitions (Figure 1) is related to the change in resistance of the discharge phases. The resistance of $Li_3Fe_2S_4$ is much greater than that of FeS_2 and Li_2FeS_2 which explains the shape of the curve.

Performance of Plasma-Sprayed Pyrite

Initial results with the HVOF system were not successful in that it was not possible to provide a sufficiently reducing atmosphere to prevent oxidation of FeS_2. XRD analysis showed that the deposits consisted primarily of Fe_2O_3 with minor amounts of pyrite, pyrrhotite ($Fe_{1-x}S$), and greigite (Fe_3S_4). The lower-sulfide phases are undesirable due to their much lower emfs of ~1.25 V at 500°C (vs. LiSi) compared ~2.0 V for pyrite.

The HVOF technique was abandoned in favor of plasma spraying using a dc arc under argon. Initial test results showed reasonably good adhesion of the deposit to the substrate. A photomicrograph of a cross-sectioned sample is shown in Figure 2. The deposited material was relatively dense and XRD analysis showed the primary phase to be troilite (Fe_7S_8), rather than pyrite. The discharge trace for a representative sample of

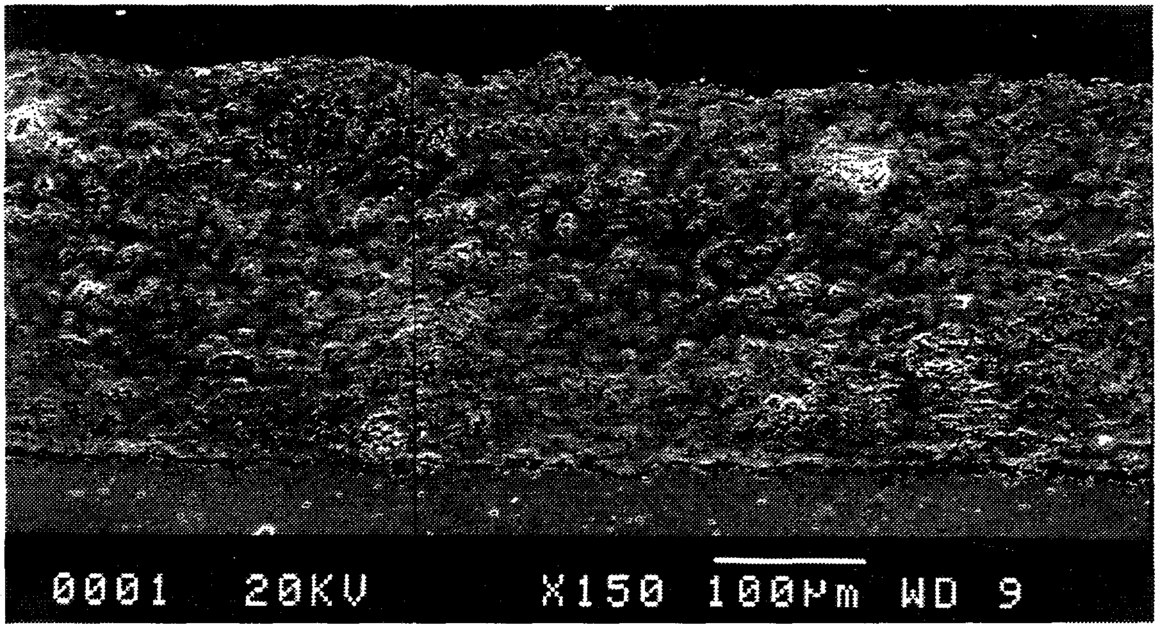

Figure 2. Cross-Sectioned Sample of Early Deposit Identified by XRD as Troilite.

this material (0.122 g, 0.0012" thick) is shown in Figure 3. The elevated voltage during open circuit at the start of the test was due to oxidized Fe species and possibly sulfur. However, there was no upper-voltage plateau present when the cell was placed under load. Only the lower-voltage plateau for the FeS-containing phase was evident. This is consistent with the XRD data for the presence of troilite and the absence of pyrite. The resistance of the cell was comparable to that of the cell with natural pyrite, even though the resistivity of the troilite is higher than that of pyrite. The improved contact of the deposit with the substrate may be responsible for this.

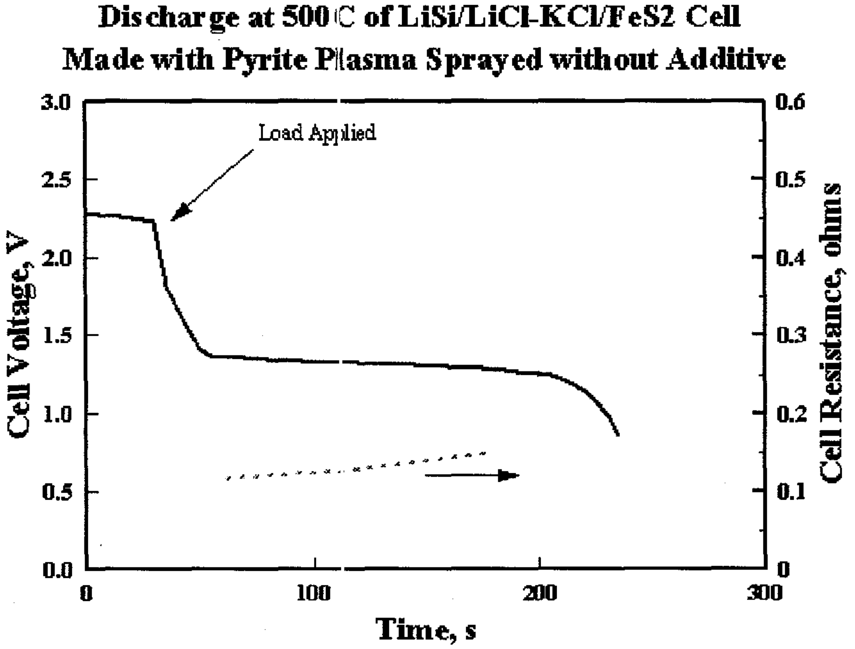

Figure 3. Discharge of Single Cell Made with Plasma-Sprayed Pyrite Containing Troilite.

Several tests were conducted in which a proprietary thermal-moderating additive was blended with the pyrite and then ball milled before injection into the plasma. The intent was to aid in processing and, more importantly, to suppress thermal decomposition of the pyrite. The tests were successful, in that XRD examination of a number of deposits prepared under these conditions showed the major phase to be pyrite, with only a minor amount of pyrrhotite.

The results of single-cell tests with this material are summarized in Figure 4 for a deposit mass of 0.1983 g (0.002" thick). The initial voltage transient was still evident from electroactive impurities with a higher emf then FeS_2, but a well-defined upper plateau was now evident, which corroborates the XRD data. It is obvious from the results of these tests that the thermal moderator was successful in minimizing thermal decomposition and obtaining the desired stoichiometry during plasma spraying of pyrite.

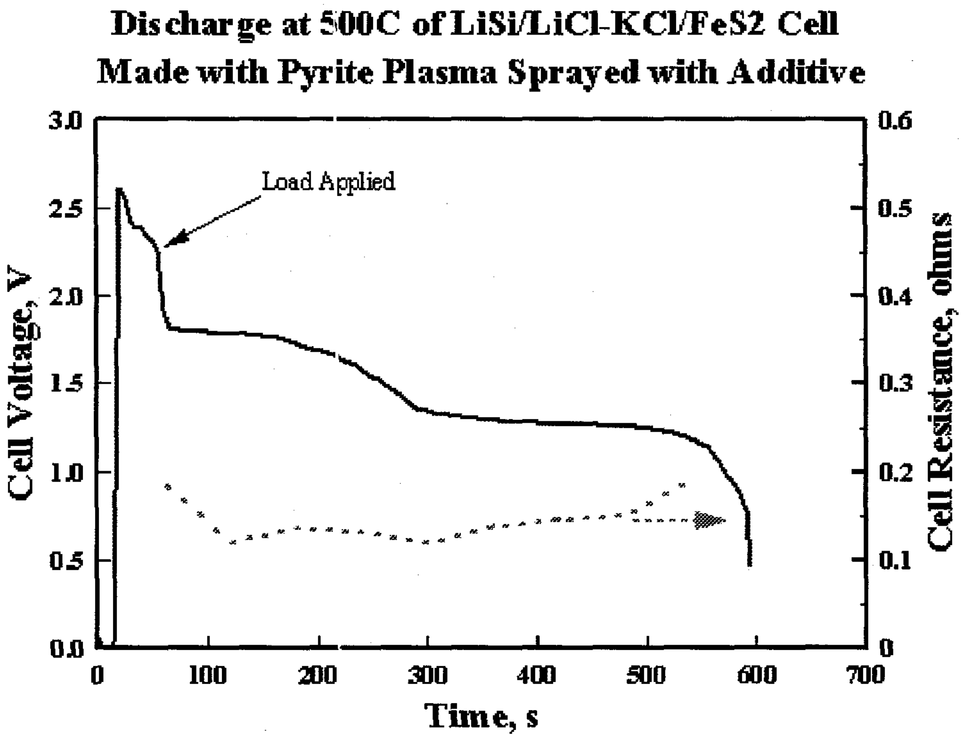

Figure 4. Discharge of Pyrite Plasma-Sprayed in Presence of Additive to Suppress Thermal Decomposition.

The resistance of the cell was initially higher but dropped quickly to that of the standard cell as discharge progressed. The initial higher resistance may be due to poor wetting of the sample at the start of discharge. The low-porosity substrate doesn't allow immediate access of electrolyte to the rear of the sample. The resistance of this cell paralleled that observed for the cell with natural pyrite, except that it did not change as dramatically at the phase transitions—especially at the end of discharge. The much higher resistance in the latter case may reflect a reduction in particle-particle contact during discharge which is absent in the case of the monolithic plasma-sprayed deposit which has improved interfacial contact with the stainless steel current collector.

The capacities to a cutoff voltage of 0.5 V of the plasma-sprayed materials deposited in the presence of the thermal moderator ranged from 2,760-2,938 coulombs/g which was comparable to that for the conventional cathode of 2,740 coulomb/g. On a volumetric basic, however, these plasmas-sprayed cathodes delivered 69,000 coulombs/cm^3 compared to only 7,950 coulombs/cm^3 for the standard cathode—a factor of almost 9 greater. These preliminary results are very encouraging.

The data from Figures 1 and 4 are normalized on a sample mass basis and are presented in Figure 5 for the steady-state voltage, after correcting for the open-circuit time. The voltage for the pyrite plasma sprayed in the presence of the thermal moderator tracks that of the natural pyrite quite well and is actually slightly higher after the major voltage transition. This indicates lower polarization for this material. Comparable data are presented in Figure 6 for the cell resistance. The resistance hump normally seen with cells with cold-pressed cathodes is conspicuously absent for the plasma-sprayed materials.

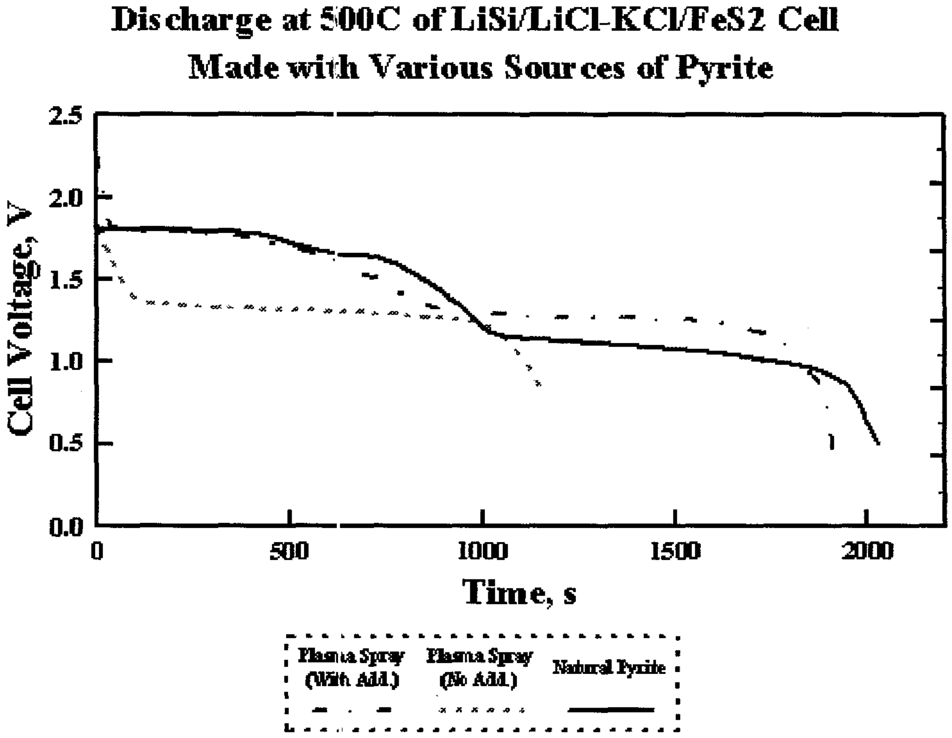

Figure 5. Comparison of Discharge Behavior of Cells for Various Pyrite Sources.

DISCUSSION

Conventional cold-pressed cathodes contain only 70-75% by weight of active pyrite. Thus, the phase purity of the plasma-sprayed pyrite deposit can be low as this and still provide a comparable capacity. Since plasma spraying is done by a robotic arm under computer control, it should be easy to scale up to a continuous process for commercial production of parts. This makes this technology attractive and potentially more cost effective than the labor-intensive powder-pressing operations.

While the preliminary results obtained with dc-arc plasma spraying are favorable, there are several areas that merit more attention. The optimum spraying conditions still

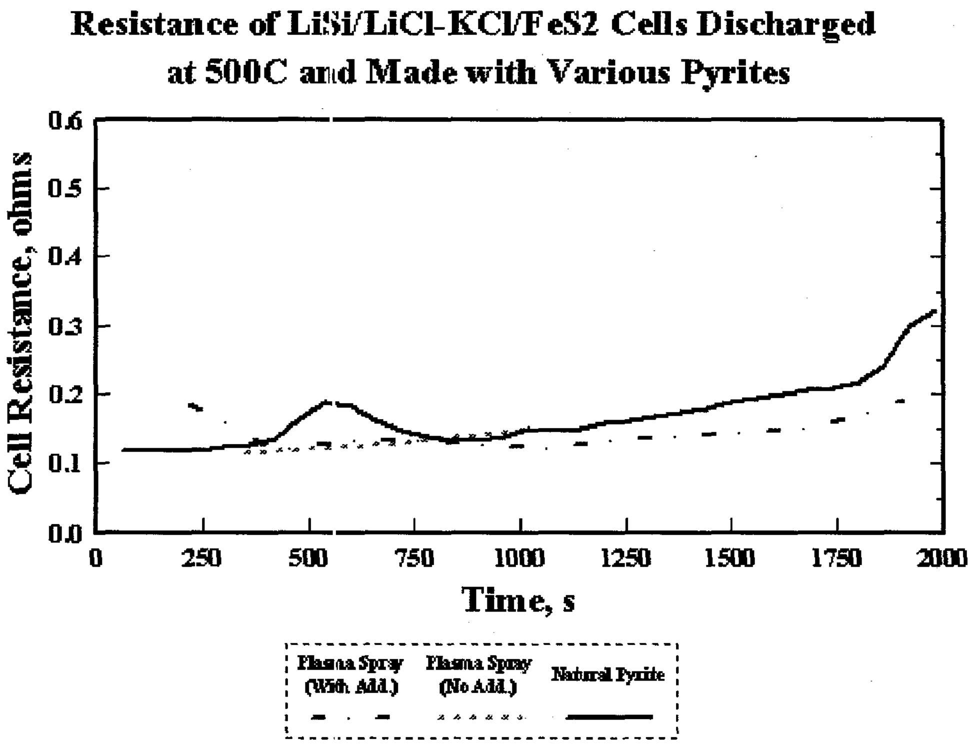

Figure 6. Cell Resistances of Single Cells Discharged at 500°C for Various Sources of Pyrite.

need to be defined which includes the morphology of the pyrite feed material. The use of nanostructured pyrite could greatly improve the properties of the deposit. The one possible disadvantage of using a dense pyrite film has to do with the potentially limited surface area available relative to that of a pressed-powder pellet made with a very fine pyrite. During the start of discharge, only the geometric area of the pyrite deposit may be readily available electrochemically, with the rear not being initially accessible. This is not a problem with pressed-pellet cathodes and may not pose a problem with plasma-sprayed pyrite during long discharges. One way to mitigate this problem would be to induce porosity into the deposit. This would allow electrolyte from the separator to access more of the pyrite and increase the effective current density possible.

CONCLUSIONS

The use of HVOF with pyrite feed material and a 304 stainless steel substrate results in unacceptable oxidation and the formation of Fe_2O_3 along with lower sulfides of iron (pyrrhotite and greigite) which have a much lower emf vs. LiSi than pyrite. Plasma spraying with a dc arc under argon results in the formation of troilite, another lower sulfide of iron, which has an emf similar to the other lower iron sulfides. Under these conditions, the decomposition of pyrite is extreme. However, by incorporation of a thermal moderator into the pyrite feed, the thermal decomposition of pyrite is suppressed. Thin (0.2 - 4.5 mils) films of predominantly pyrite are obtained that show reasonably good electrochemical behavior at 500°C in single-cell tests at 125 mA/cm^2 load with 1-s pulses of 250 mA/cm^2 every minute. Cell resistances were comparable during initial discharge and slightly lower deeper into discharge than those of the standard cell with pressed-powered cathodes. The hump in cell resistance during discharge due to formation of $Li_3Fe_2S_4$ is absent with plasma-sprayed pyrite and may be a result of the enhanced electrical conductivity over powder compacts. More work is needed to optimize the deposition conditions and to impart additional porosity into the pyrite deposits to increase their rate capability.

ACKNOWLEDGMENTS

Sandia National Laboratories is a multiprogram laboratory operated by Sandia Corp, a Lockheed-Martin company, for the United States Department of Energy under Contract DE-AC04-94AL85000.

REFERENCES

1. S. K. Preta, Z. Tomczuk, S. von Winbush, and M. F. Roche, J. Electrochem. Soc., **130**, 264 (1983).
2. Z. Tomczuk, B. Tani, N. C. Otto, M. F. Roche, and D. R. Vissers, J. Electrochem. Soc., **129** (5), 925 (1982).